Dogan, A. H., Zus, F., Dick, G., Wickert, J., Schuh, H., Durdag, U. M., Erdogan, B. (2024): Improving the wet mapping function by numerical weather models. - Advances in Space Research, 73, 1, 404-413.

https://doi.org/10.1016/j.asr.2023.07.060

Improving the Wet Mapping Function by Numerical Weather Models

Ali Hasan Dogan[1,2*], Florian Zus[1], Galina Dick[1], Jens Wickert[1,3], Harald Schuh[1,3], Utkan Mustafa Durdag[4] and Bahattin Erdogan[2]

[1]GFZ German Research Centre for Geosciences, Telegrafenberg, 14473 Potsdam, Germany

[2]Department of Geomatic Engineering, Faculty of Civil Engineering, Yildiz Technical University, 34220 Istanbul, Türkiye

[3]Technische Universität Berlin, 10623 Berlin, Germany

[4]Department of Geomatic Engineering, Faculty of Engineering, Artvin Coruh University, Artvin, Türkiye

Abstract

In space geodetic techniques, the mapping functions (MFs) provide the relationship between zenith and slant tropospheric delays. The MFs are determined under the assumption of spherically layered atmosphere. However, the atmosphere is not spherically layered, and the asymmetry should be considered. Therefore, tropospheric gradients are taken into account. Nevertheless, tropospheric gradients alone can not fully represent the deviation from a spherically layered atmosphere, and hence cm level errors arise especially for low elevation angles. In this study, we present new approaches to modify the wet MF to reduce mismodelling of tropospheric delays. The delays in the study were calculated using ray-tracing algorithm based on ECMWF's ERA5 dataset. We first analyzed the performances of the new approaches. Then, two Precise Point Positioning (PPP) simulation studies and a real case study were carried out for two different regions namely Germany and Türkiye. According to the results, the proposed approaches reduce the modelling errors up to by a factor 6 for both regions. Besides, simulation studies show that the approaches improve the accuracies of the ZTDs and heights. In the practical application however, we could not find a clear improvement in the PPP analyze and this might be related to the ERA5 which can not be regarded error-free.

Keywords: Tropospheric delay, Mapping Function, Numerical Weather Model, ERA5, PPP

Corresponding Author:

Ali Hasan Dogan

dogan@gfz-potsdam.de / alihasan@yildiz.edu.tr

+90 212 383 5322

Introduction

GNSS (Global Navigation Satellite Systems) is the most widely used space geodetic technique for positioning, navigation and timing since it works in all weather conditions and 24 hours a day. The basic GNSS measurement is the signal travel time between the navigation satellites and the receiving ground station. Thereby the signals are passing through the Earth's atmosphere. The neutral part of the atmosphere, simply referred to as the troposphere, causes signal delays due to the dry air and water vapor. These delays, namely tropospheric delays, can reach up to 30 m especially at lower elevation angles, and hence must be considered in the processing step in order to achieve precise positioning and timing information (Teunissen and Montenbruck, 2017). Tropospheric delays are typically divided into hydrostatic and wet delays. Although the Zenith Hydrostatic Delay (ZHD) can be accurately obtained using the pressure value of the station by the equation of Saastamoinen (1972) or Davis et al. (1985), Zenith Wet Delays (ZWD) cannot be calculated accurately due to the rapid changes of the humidity field in the atmosphere both temporally and spatially (Landskron and Böhm, 2018a). Thus, the ZWD must be modelled in space geodetic techniques. Tropospheric delays occur in any slant direction. In the GNSS analysis however, these delays are estimated in the zenith direction. The relation between slant and zenith delays is provided by the Mapping Functions (MFs) for a layered atmosphere. The MFs are determined based on the atmospheric parameters in a vertical profile. Radiosonde (RS) and Numerical Weather Model (NWM) data can be used to obtain the required parameters (Niell, 2001; Böhm and Schuh, 2004). It was demonstrated that compared with MFs derived from a climatology, MFs derived from NWMs increase the accuracy of the estimated parameters in the analysis of space geodetic (Böhm and Schuh, 2004; Böhm et al., 2006a). Typically, the hydrostatic and wet MF are calculated under the assumption of a spherically layered atmosphere by using ray tracing algorithms (see e.g., Zus et al., 2014). The atmosphere however, is not symmetric and, the azimuthal asymmetry must be considered. In space geodetic techniques, the so-called tropospheric gradients take into account the effect of azimuthal asymmetry (Chen and Herring, 1997; Bar-Sever et al., 1998; Willis et al., 2012). The estimation of the tropospheric gradients is important especially if low-elevation angle observations are included in the analysis (Nilsson et al., 2013). Low elevation angle observations are important insofar as they improve the decorrelation of otherwise strongly correlated parameters such as the zenith delay, station height and station clock error (Rothacher et al. 1998). For example, Masoumi et al. (2017) demonstrated that including lower elevation observations decrease the correlations between the Zenith Total Delay (ZTD), station height and clock. On the other hand, mismodelling of the tropospheric delay or MFs causes increasing errors in station heights. One of the most used MFs in the literature based on a NWM climatology is the Global Mapping Function (GMF) (Böhm et al., 2006b). It has been derived based on spherical harmonics series by using ERA-40's monthly mean vertical atmospheric profiles given on global grid data from 1999 to 2002. Although this MF is easy-to-use and has better accuracy than the widely used Niell Mapping Function (NMF) (Niell, 1996), especially short-term variations cannot be predicted since GMF is based on climatology data. The Vienna Mapping Functions 1 (VMF1) however, is generated based on European Centre for Medium-Range Weather Forecasts (ECMWF) operational NWM analysis on a global 2°x2.5° grid with 6-hour temporal resolution. Tesmer et al. (2007) have shown that the VMF1 is more accurate than the GMF and NMF due to the fact that it is based on NWM data. Moreover, there are other MFs which were produced based on the VMF1 concept such as the UNB-VMF1 (Santos et al., 2012; Urquhart et al., 2014) and the GFZ-VMF1 (Zus et al., 2015). The main difference between these MFs is that they are based on different NWM data. They all have in common that they are based on an efficient concept, i.e., the number of MF coefficients to be derived from the NWM are kept minimal. Other more rigorous solutions exist such as direct mapping or the derivation of additional (all three) MF coefficients such as the Potsdam Mapping Function (PMF) (Zus et al., 2014).

The choice of MF does not only affect the coordinates but also the ZTDs because of the high correlation between them. The ZTD estimates are the main observable in GNSS based atmospheric remote sensing because the Precipitable Water Vapor (PWV), a key quantity in meteorology, can be derived with very little additional uncertainty (Bevis et al., 1992). Recently, Zus et al., (2021) proposed an approach to modify the wet MF and to reduce the errors of estimated heights and ZTDs. They showed that a simple modification of the wet MF reduced the errors from the standard approach from 2.4 mm to 1 mm and 1.8 mm to 0.5 mm for heights and ZTDs, respectively.

Here, we propose and test three approaches to modify the wet MF. The corresponding performance of the modified wet MFs is analyzed. Simulation studies and a case study with real GNSS data were carried out for two different European regions based on Precise Point Positioning (PPP) technique proposed by Zumberge et al. (1997). The first one covers Central Europe including Germany and large parts of Poland, Czech Republic and Austria, and the second covers Türkiye.

Tropospheric Delay

In space geodetic techniques, the troposphere causes signal delays due to the dry air and water vapor. The tropospheric delay T is defined as;

$$T = \int_S n(s)\, ds - G \qquad (1)$$

where s denotes the arc length of the ray path, n represents the refractive index and G denotes the geometric distance between the GNSS satellite and the ground receiver. The refractive index is related to refractivity N, hence T can be written based on hydrostatic and wet refractivity as;

$$n = 10^{-6}N + 1 \qquad (2)$$

$$T = 10^{-6}\int_S N_h(s)\, ds + 10^{-6}\int_S N_w(s)\, ds + S - G \qquad (3)$$

where S is the length of the actual propagation path of the ray from the GNSS satellite to the ground station. N_h and N_w are the refractivities of the hydrostatic and wet part, respectively. The refractivity is a function of pressure, temperature and water vapor pressure. In order to determine the refractivity, data from radiosondes and numerical weather models can be used. RS only provides profile information at dedicated times (typically two times per day). On the other hand, NWMs provide the three-dimensional refractivity field. In this study we are especially interested in the deviation from a locally spherically layered atmosphere and thus data from RS are not useful. We make use of ECMWF's ERA5 reanalysis, which provides atmospheric variables globally with both high temporal (1-h) and spatial (0.25°) high resolution (Hersbach et al., 2020). It is important to note that NWMs do not represent the true state of the troposphere. They can be solely regarded an approximation of it.

The hydrostatic and wet refractivity are computed according to;

$$N_h = k_1 \frac{M_d}{R}\rho \qquad (4)$$

$$N_w = k_2' \frac{\mathrm{e}}{T} + k_3 \frac{\mathrm{e}}{T^2} \qquad (5)$$

where k_1, k_2' and k_3 are empirically determined refractivity constants (Thayer, 1974). M_d is molar mass of dry air, R is general gas constant, e denotes water vapor pressure and T denotes temperature. ρ represents total density and can be calculated as;

$$\rho = \rho_d + \rho_w \qquad (6)$$

$$\rho_d = (p - \mathrm{e})\frac{M_d}{R}\frac{1}{T} \tag{7}$$

$$\rho_w = \mathrm{e}\frac{M_w}{R}\frac{1}{T} \tag{8}$$

where ρ_d and ρ_w denote partial densities of dry and wet part, respectively. p is pressure and M_w is molar mass of water.

The delays for the hydrostatic and wet parts, hereinafter denoted T_h and T_w, are defined as in Eq. (9) and Eq. (10). These delays are determined by a ray-tracing algorithm. In this study, we followed the algorithm proposed by Zus et al. (2014).

$$T_h = 10^{-6}\int_S \; N_h(s)\,ds + S - G \tag{9}$$

$$T_w = 10^{-6}\int_S \; N_w(s)\,ds \tag{10}$$

In space geodesy, the signal travel time is measured between the source and the receiving antenna, and this travel time is expressed in units of meter using the speed of light (Nilsson et al., 2013). In the analysis of space geodetic measurements, solely corresponding delays in zenith direction are estimated. The relation between slant and zenith delays is provided by the so-called Mapping Function (MF). MFs are determined using Herring's (1992) continued fraction form (Eq. 11). MF coefficients, a, b and c, are estimated using non-linear least square estimation. In this study, we followed the same strategy as in Zus et al. (2021) with only small modification in the quality check step.

$$\mathrm{MF}(e) = \frac{1+\frac{a}{1+\frac{b}{1+c}}}{\sin(e)+\frac{a}{\sin(e)+\frac{b}{\sin(e)+c}}} \tag{11}$$

We note that MFs derived from a layered atmosphere depend on the elevation angle e only. The MFs do not depend on the azimuth angle α. Typically, tropospheric delays which are calculated under the assumption of a spherically layered atmosphere, hereinafter denoted T_0, are used to estimate the MF coefficients. Another possibility is to compute a bunch of tropospheric delays for various elevation and azimuth angles, average over the azimuth angle, and estimate the MF coefficients. However, those MF coefficients will differ from MF coefficients obtained by utilizing tropospheric delays calculated under the assumption of a spherically layered atmosphere. The azimuthal asymmetry is approximated utilizing tropospheric gradients, hereinafter denoted G_N and G_E, using the model by Chen and Herring (1997). Hence, the tropospheric delay model can be written as;

$$T(e, a) \cong T_0(e) + m_g(e)[G_N \cos\alpha + \; G_E \sin\alpha] \tag{12}$$

$$T_0(e) = m_h(e)Z_h + m_w(e)Z_w \tag{13}$$

$$m_g(e) = \frac{1}{\sin(e)\tan(e)+C} \tag{14}$$

where Z_h and Z_w are hydrostatic and wet delays in zenith direction; m_h and m_w are hydrostatic and wet mapping functions and, m_g denotes the gradient mapping function. C in Eq. (14) has a value of 0.0031 and 0.0006 for the hydrostatic and wet part, respectively (Chen and Herring, 1997).

In this study, we compute 120 tropospheric delays for each station and each epoch. The delays were computed under the 30° spacing azimuth angles, and in each azimuth we considered the elevation angles as 3°, 5°, 7°, 10°, 15°, 20°, 30°, 50°, 70°, and 90°. In addition, we calculate 10 delays utilizing solely the refractivity profile above the station in question. Those 10 tropospheric delays, i.e., tropospheric delays calculated under the assumption of a spherically layered atmosphere, are the ones we utilize in the determination of the hydrostatic and wet MF coefficients. For details the reader is referred to Zus et al. (2021).

Modified Wet Mapping Function

In the GNSS analysis, the tropospheric delay is modeled based on Eq. 12. However, the right-hand side in Eq. 12 is only an approximation of the tropospheric delay. In literature various variants exist to refine the approximation of the tropospheric delay. In general, the azimuth and elevation angle dependency of the tropospheric delays can be approximated by a polynomial expansion. For example, the rigorous expansion of the tropospheric delay utilizing orthogonal polynomials was proposed by Zhang et al. (2020) and Barriot and Feng (2021). Another approach which is presumably less accurate but more simple was proposed by Landskron and Böhm (2018b). In this study we follow an approach which is very close to the approach proposed by Landskron and Böhm (2018b). We will follow the approach by Zus et al. (2021). For some elevation angles the differences between tropospheric delays and tropospheric delays calculated under the assumption of a spherically layered atmosphere are expanded in a Fourier series. If one further assumes that the coefficients of the Fourier series follow the same elevation angle dependency, namely the elevation angle dependency of the gradient MF, then the tropospheric delay reads as;

$$T(e,a) \cong m_h(e)Z_h + m_w(e)Z_w + m_g(e)Z_0 + m_g(e)[G_N \cos\alpha + G_E \sin\alpha] + m_g(e)[Z_1 \cos 2\alpha + Z_2 \sin 2\alpha] + m_g(e)[Z_3 \cos 3\alpha + Z_4 \sin 3\alpha] + \cdots \quad (15)$$

As it can be seen in the equation, G_N and G_E can be interpreted as the second and third coefficients of the series expansion. The first coefficient of the series expansion Z_0 appears in a term which depends solely on the elevation angle. Hence, Zus et al. (2021) suggested to modify the wet MF as follows.

$$z' = \frac{Z_0}{Z_w} \quad (16)$$

$$m_w^*(e) = m_w(e) + m_g(e)z' \quad (17)$$

After the modification of the wet MF, the tropospheric delay can be written as;

$$T(e,\alpha) \cong m_h(e)Z_h + m_w^*(e)Z_w + m_g(e)[G_N \cos\alpha + G_E \sin\alpha] \quad (18)$$

In other words, the wet MF which still depends on the elevation angle only, takes into account the deviation from a spherically layered atmosphere. Based on the PPP simulation results presented in Zus et al. (2021), it can be concluded that the modification of the wet MF can significantly reduce the errors of the estimated zenith delays and heights. However, they used C as 0.0031 in gradient MF at the modification step. Since the origin of the extra term containing Z_0 is more likely to be the wet than the hydrostatic refractivity field a different choice of C appears natural. Therefore, we chose C as 0.0006 in order to improve the approximation. Hence, we modified Eq. (17) as;

$$m_w^*(e) = m_w(e) + m_g'(e)z'' \quad (19)$$

In m_g', C was taken as 0.0006.

As stated in the above section, hydrostatic and wet MF coefficients are typically determined utilizing tropospheric delays calculated under the assumption of spherically layered atmosphere. This is the case for e.g. the VMF1 (Böhm et al., 2006a) where the parameter b and c are fixed to known values and solely the parameter a is determined based on a single ray-traced delay. Zus et al. (2015) analyzed the error of this concept. They showed that the differences between the VMF1 concept and the more rigorous approach are small in general. However, they can become substantial when the station height is different from the station height for which the single coefficient was determined. Hence, we estimated station specific MF coefficients by direct mapping to avoid the errors for low-elevation observations.

The tropospheric gradients were obtained based on Zus et al. (2019). To modify the wet MF, we first obtained the differences D between T and T_0 by averaging over the azimuth angles. Then we approximated the differences D, which depend on the elevation angle by an elevation angle dependent function of our choice and obtained by a least square fit the parameters of our chosen functional form. Hereby low elevation angle differences are down-weighted by the square of the sine of the elevation angle. We compared three approaches to modify wet MF. They are summarized in Table 1.

Table 1 The three proposed approaches to modify the wet MF.

Approach	Description	Observation Model	Modified Wet MF
(i)	suggested by Zus et al. (2021)	$D(e) \cong m_g(e)z_0$	$m_w^i(e) = m_w(e) + m_g(e)\dfrac{z_0}{Z_w}$
(ii)	same as (i) with different C	$D(e) \cong m'_g(e)z_0$	$m_w^{ii}(e) = m_w(e) + m'_g(e)\dfrac{z_0}{Z_w}$
(iii)	combination of (i) and (ii)	$D(e) \cong m_g(e)z_1 + m'_g(e)z_2$	$m_w^{iii}(e) = m_w(e) + m_g(e)\dfrac{z_1}{Z_w} + m'_g(e)\dfrac{z_2}{Z_w}$

Results and Discussion

The ECMWF's atmospheric reanalysis ERA5 was used to calculate zenith delays, estimate MF coefficients, gradients and additional tropospheric parameters. We assume that ERA5 represents the true atmospheric conditions. Although it can provide atmospheric variables globally, the accuracy of variables varies from area to area. For example, Jiao et al. (2021) investigated the spatial-temporal variation performance of ERA5 precipitation data over China. They found that correlations between ERA5 and observations vary from region to region due to the topography. Velikou et al. (2022) showed that the temperature accuracy of ERA5 changes for different regions in Europe. Therefore, we selected two different study areas as Germany and Türkiye, to test the proposed approaches. In both regions, we selected real continuously operating GNSS stations (Fig. 1 and Fig. 2). In the figures, blue stars indicate the stations POTS and ISTN which were used in the second simulation studies for validation and the green triangles denote the stations that we utilized in the case study. In the case study, we also used the stations POTS and ISTN. The stations shown in the figures were used in the first simulation study. The stations cover Germany and Türkiye so that our results can be regarded representative for stations located in the respective country. Since significant deviations from a locally spherically layered troposphere can be expected in warm and moist seasons, the time period was chosen as July 2021.

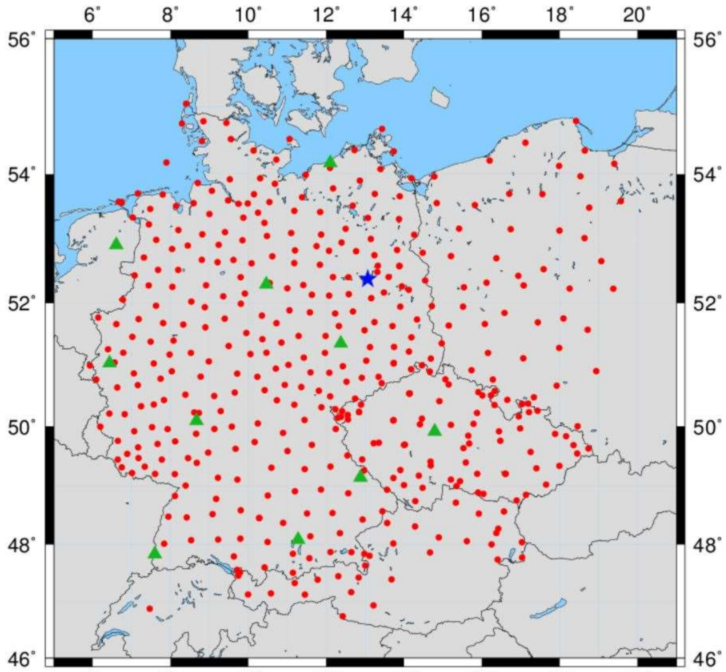

Fig. 1 GNSS stations located in central Europe covering Germany and large parts of Poland, Czech Republic and Austria. Blue star represents station POTS, green triangles denote the stations utilized in the case study. In total, there are 431 stations.

Fig. 2 GNSS stations located in Türkiye. Blue star represents station ISTN, green triangles denote the stations utilized in the case study. In total, there are 159 stations.

At first, we calculated ray-traced tropospheric delays utilizing the algorithm proposed by Zus et al. (2014). Next, we estimated the MF coefficients, gradients and additional tropospheric parameters for each station and for each hour. We then investigate the difference between ray-traced and assembled tropospheric delays. The assembled tropospheric delays follow from the combination of zenith delays, MF coefficients, gradients and additional tropospheric parameters. We investigate the three approaches mentioned above. We determined the residuals for each station, epoch, elevation and azimuth angles, and then we calculated the RMS deviations for each elevation angle. In Fig. 3, the RMS deviations as a special function of the elevation angle (which is close to the gradient MF) are shown for both regions using all stations in the regions. We also plotted the RMS deviations for the traditional (standard) approach. The traditional approach, given in Eq. (12), was represented by “D” in the figure. The reason of choosing the special function of the elevation angle and not the elevation angle itself becomes clear in this plot as the RMS deviation for the standard approach nearly follows a straight line. This explains why it is nearby to choose simply the gradient MF times a factor to improve the functional form of the tropospheric delay. It can be seen that the proposed approaches summarized in Table 1 decrease the errors in both regions especially for low elevation angles. For example, at the lowest elevation angle of three degree the approach **(i)** (see Table 1) decreases the error of the standard approach by a factor of three and the approach **(ii)** decreases the error of the standard approach by a factor of six. The approach **(iii)** decreases the error of the standard approach to a few mm for all elevation angles. These improvements have a critical importance since adding low elevation observations in the positioning analysis decrease the correlation between the unknowns.

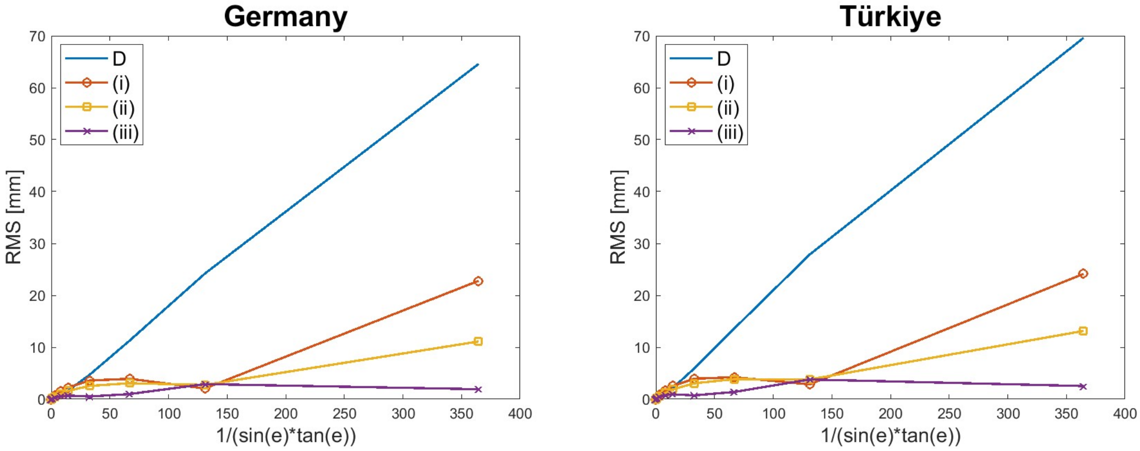

Fig. 3 RMS deviation as a special function of the elevation angle for the approaches. The left plot shows the result for Germany the right plot shows the result for Türkiye. For details the reader is referred to the text.

The additional parameters which are used to modify the wet MF are related to the humidity field. In order to show this relation, we plotted the PWV, G_N, G_E and the parameter Z_0 for one epoch in Fig. 4. The PWV and Z_0 values in the figure were derived for a grid with a horizontal resolution of 0.5°. It is obvious that the Z_0 values are not random numbers, they are related to the humidity field. Roughly spoken, the Z_0 values arise in the convergence zone of the (integrated) water vapor field. In essence, the tropospheric gradients (G_N and G_E) are related to the first derivative in the PWV field and the parameter Z_0 is related to the second derivative in the PWV field. The appearance of Z_0 can also be roughly translated into an error of estimated ZTDs in PPP. According to the rule of thumb of Zus et al (2021), the error in the ZTD estimates is about seven times Z_0. The Z_0 values range from -2 mm to 2 mm, and this corresponds to errors in the ZTD estimates of about -14 mm to 14 mm. Therefore, they should be taken into account in the modelling of the delays. However, the filigree structure in the Z_0 map is an indication that NWMs may have problems to predict this additional parameter. Small deviations of the NWM from the true state of the atmosphere can cause significantly different Z_i values. Hence, although we clearly improve the functional form of the tropospheric delay by a simple approach it is not guaranteed that this will yield an improvement in a practical application. The success in practice will depend on the ability of the NWM, in our case ERA5, to constrain the additional tropospheric parameters.

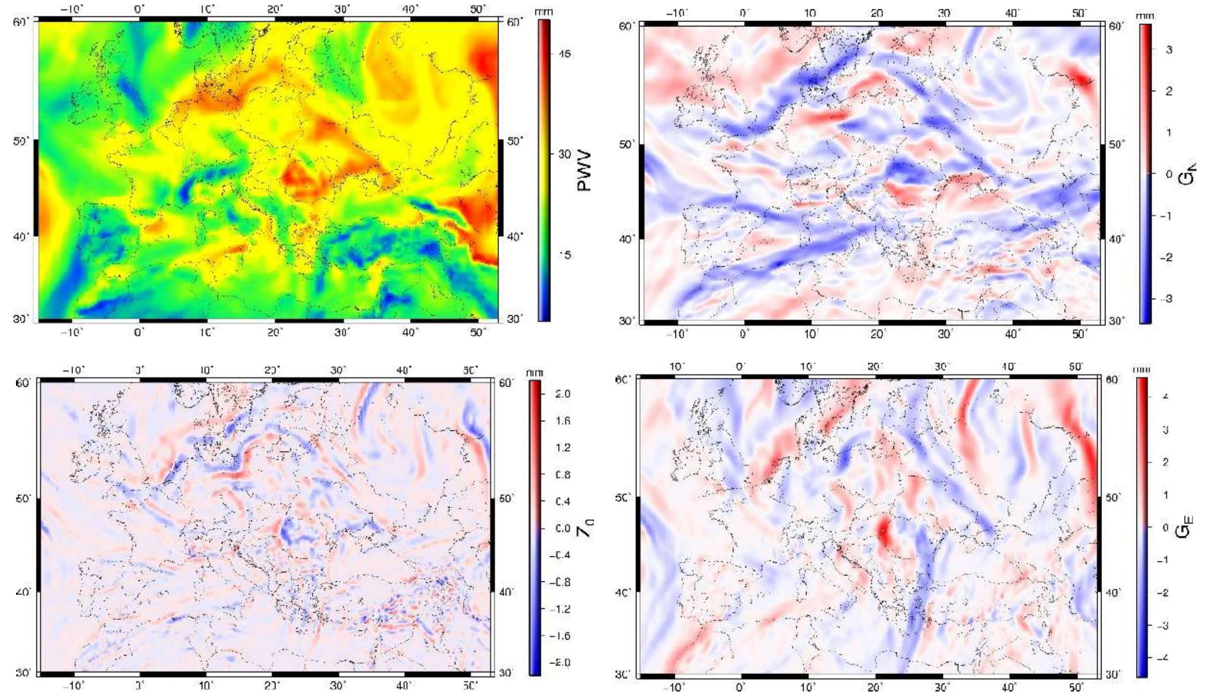

Fig. 4 The regional PWV, G_N, G_E and the additional parameter Z_0 that is used to modify the wet MF for July 1, 2021 07 UTC (first approach)

In the next step a first simulation study was carried out to test the standard and proposed approaches for the stations in the considered regions. In the first PPP simulation study, the so-called linearized observation equation was solved and coordinates, clocks zenith delays and tropospheric gradients were estimated. Other GNSS error sources and parameters such as ambiguities were assumed as fixed. Details on the PPP simulation are explained in Zus et al. (2021). In the PPP simulation, ray-traced tropospheric delays were used as observations, and estimated coordinates, zenith delays and gradients were compared with the known values. We ran five scenarios to demonstrate the potential of the new approaches in PPP. The scenarios are listed in Table 2. In the first scenario, the ZHD was taken from Global Pressure and Temperature (GPT) model (Böhm et al., 2007) and the hydrostatic and wet MF were taken from GMF (Böhm et al., 2006b). In the second scenario, the a priori ZHD and the MFs were based on the NWM. In the third, fourth and fifth scenarios, again all parameters were based on NWM. However, the wet MFs were modified based on the proposed approaches of this study.

Table 2 Scenarios in the PPP simulation. The scenarios differ by the a priori ZHD, hydrostatic and wet MF that is utilized in the simulation.

Scenario	**ZHD**	**MF_H**	**MF_w**
1	GPT	GMF	GMF
2	NWM	PMF	PMF
3	NWM	PMF	$PMF_{(i)}$
4	NWM	PMF	$PMF_{(ii)}$
5	NWM	PMF	$PMF_{(iii)}$

The quality of the tropospheric model is measured in terms of the station specific RMS values. The average RMS error for the estimated station Up component and ZTD is summarized in Table 3. In the first scenario, we utilize data from climatology and thus as to expect, the largest RMS errors were obtained for both regions. In the second scenario, the RMS errors decreased from 4.4 mm to 2.5 mm and 5.2 mm to 4.0 mm in the Up component for the stations located in Germany and Türkiye, respectively. Similarly, the RMS values decreased from 2.2 mm to 1.5 mm and 2.5 mm to 2.0 mm in the ZTD. In the other scenarios, we only changed the wet MFs. It can be seen from the table that the proposed approaches improve the ZTD accuracy to a sub-mm level in both regions. Moreover, the accuracies of the Up component were improved by approximately 70% in these regions.

Table 3 RMS values of the scenarios in the PPP simulation. The time period is July 2021. The RMS values for the two regions (Germany and Türkiye) are obtained by averaging the station specific RMS errors.

Scenario	Germany		Türkiye	
	ZTD [mm]	Up [mm]	ZTD [mm]	Up [mm]
1	2.2	4.4	2.5	5.2
2	1.5	2.5	2.0	4.0
3	0.5	0.9	0.5	1.4
4	0.4	0.7	0.5	1.2
5	0.3	0.7	0.4	1.2

We then carried out a second simulation study to test the new approaches in an environment that is closer to the real-world application. In essence, we generated simulated code and carrier phase observations for L1 and L2 signals based on real satellite geometry for one station in the respective region, using Bernese v5.2 (Dach et al., 2015). We utilized only the GPS constellation. In order to generate more realistic observations, we added normally distributed random errors to the observations. A priori sigmas were chosen to be 50 cm and 2 mm for code and carrier phase observations, respectively. Moreover, we considered atmospheric (van Dam and Ray, 2010) and ocean loading corrections (Lyard et al., 2006; URL-1). The simulation study also includes Earth rotation parameters and differential code biases. For the ionospheric effects, we used CODE's global ionosphere maps. Finally, tropospheric delays were added based on the ray tracing algorithm.

We selected the stations POTS (in Potsdam, Germany) and ISTN (in Istanbul, Türkiye). The simulated observations were processed based on PPP technique using Bernese v5.2. In the processing step, a priori ZHD and MFs were altered as summarized in Table 2. For each scenario, we calculated residuals of the parameters of PPP analysis. Then, we computed standard deviations of the parameters which are listed in Table 4. As in the first simulation study, the worst results were obtained in the first scenario in which data from climatology are utilized. In the second scenario, we used the NWM based ZHD and MFs to process observations. Using NWM based parameters slightly reduce the errors. The three newly proposed approaches yield the same precisions in the ZTD and the Up-component for both regions. The approaches decreased the errors especially w.r.t the first scenario. The improvements are 6% and 4% in ZTD, and 7% and 9% in the Up-component for POTS and ISTN, respectively.

Table 4 Standard deviations of the parameters in the second simulation study

Scenario	Germany (POTS)		Türkiye (ISTN)	
	ZTD [mm]	Up [mm]	ZTD [mm]	Up [mm]
1	4.9	4.6	4.9	4.4
2	4.8	4.4	4.9	4.2
3	4.6	4.3	4.7	4.0
4	4.6	4.3	4.7	4.0
5	4.6	4.3	4.7	4.0

It is important to note that only ray-traced tropospheric delays were used as observations without any noise, and solely coordinates, ZTDs, clock errors and gradients were estimated in the first simulation study utilizing a quasi-realistic observation geometry. In the second simulation study however, other GNSS error sources (e.g., noise on the carrier phase and code observation and the ambiguity) are taken into account in the generation of observations and in the PPP analysis. Thus, improvements of the proposed approaches in the second simulation study appear smaller. For example, if in the first simulation study we chose the GPS only geometry and if gradients are solely estimated on a daily basis (as it is the case in the second simulation study), then the RMS error for e. g. the scenario 1 and Germany increases to 3.0 mm and 5.1 mm for the ZTD and station Up-component, respectively.

According to the results of both simulation studies, it can be concluded that the approaches to modify the wet MF improve the accuracy of the ZTD and Up-component. Although there are no significant differences between the proposed approaches in the PPP simulations, the most accurate results measured in terms of the difference between ray-traced and assembled tropospheric delays can be obtained by the approach **(iii)** proposed in this study. The results from the previous simulation studies provide us an idea on what to expect in a real-world application. This is the next and final step in our study. Thus, we selected 21 stations in total in both regions and performed a PPP analysis using real observations for the validation of the proposed approaches. In the PPP analysis, we added another scenario as listed in Table 5. In the added scenario, the a priori ZHD and MFs come from the GFZ-VMF1 which is produced based on the VMF1 concept but utilizing a different NWM namely ERA5 (Zus et al., 2015). We may regard the first and second scenario in the PPP analysis as the standard approaches.

Table 5 Scenarios in the PPP analysis. The scenarios differ by the a priori ZHD, hydrostatic and wet MF that is utilized in the simulation.

Scenario	**ZHD**	**MF_H**	**MF_w**
1	GPT	GMF	GMF
2	VMF1	VMF1	VMF1
3	NWM	PMF	PMF
4	NWM	PMF	$PMF_{(i)}$
5	NWM	PMF	$PMF_{(ii)}$
6	NWM	PMF	$PMF_{(iii)}$

The PPP analysis was carried out using Bernese v5.2. In this step, daily observations of the stations were processed. First-order ionospheric effects were eliminated by the ionosphere-free linear combination of L1 and L2 signals. Data processing strategy was summarized as in Table 6. In the analysis, a priori ZHD and MFs were changed as in Table 5. For each scenario, coordinates and ZTDs were analyzed. For the validation of ZTDs, we compared the estimated values with the ZTDs derived from the ERA5. For the coordinates, we analyzed station heights only as they are mainly affected by the chosen tropospheric model. We measure the impact by analyzing the coordinate repeatability. Moreover, the median approach was applied to the time series of ZTD residuals and heights in order to exclude outliers. The median approach is one of the most reliable outlier detection methods with 50% breakdown point (Rousseeuw and Leroy, 1987; Hampel et al., 2011). In Table 7, the statistics of both, before and after the Median approach, are presented. The standard deviations after the outlier detection are given in brackets.

Table 6 Data processing strategy

Parameter	Description
Precise GNSS orbits and clocks	Produced by CODE (Dach et al., 2020)
Navigation satellite system	GPS-Only
Cut-off angle	3°
Sampling interval	300 s for observations 1h for ZTD estimation 24h for the gradients estimation
Weighting of the observations	Elevation dependent weighting $\sin^2 e$
Second-order ionospheric effect	Global Ionosphere Maps produced by CODE
Ambiguity	Float
A priori ZHD	Changed based on the scenarios given in Table 5
Mapping Functions	
Ocean loading and atmospheric loading corrections	Regarded (Lyard et al., 2006; van Dam and Ray, 2010; URL-1)

Table 7 Statistics of the PPP analysis. The values given in brackets represents the statistics after the Median approach.

Scenario	Germany		Türkiye	
	ZTD [mm]	h [mm]	ZTD [mm]	h [mm]
1	13.5 (11.6)	5.2 (5.2)	15.9 (14.5)	9.6 (9.2)
2	13.3 (11.5)	5.4 (5.2)	15.8 (14.4)	9.7 (9.3)
3	13.3 (11.5)	5.4 (5.1)	15.9 (14.5)	9.7 (9.2)
4	13.0 (11.2)	5.3 (5.2)	15.6 (14.2)	9.9 (9.5)
5	13.0 (11.2)	5.3 (5.1)	15.7 (14.2)	9.9 (9.5)
6	13.0 (11.3)	5.3 (5.2)	15.7 (14.3)	9.9 (9.4)

It can be seen in Table 7 that all three proposed approaches (Table 1) have nearly the same precisions in station heights for both regions before outliers detection. Interestingly the first scenario which is based on climatology data gives the best results in the station heights. A possible explanation is that non-tidal loading is not applied and hence the a priori ZHD from the climatology yields the best coordinate repeatability (Steigenberger et al., 2009). We can also conclude from the Table 7 that for the considered stations and timespan there is no difference between the rigorous PMF (all three MF coefficients are estimated, scenario 3) and the much more efficient VMF1 (a single MF coefficient is estimated, scenario 2). In Germany, the proposed approaches improve the precisions w.r.t the second and third scenario. In Türkiye however, the proposed approaches increase the errors in heights. One possible explanation is that the accuracy of NWMs differ from region to region (Velikou et al., 2022). In essence, ERA5 is not accurate enough to provide higher order tropospheric parameters for Türkiye but it is accurate enough to provide them for Germany. For ZTDs the best results were obtained based on the proposed approaches in both regions. This is not too surprising as the reference ZTDs are derived from ERA5. After the outliers detection, the best results for the station heights were obtained in third and fifth scenarios for Germany. For Türkiye, the first and third scenarios yield the most precise station height estimates.

Conclusions

In this study, we propose new approaches to improve the parameterization of the tropospheric delays in space geodetic techniques (e.g., GNSS) based on the modification of wet MF. We first analyzed the model accuracies of the approaches, then we carried out two different simulation studies and finally performed a case study for two different regions. The proposed approaches improve the model accuracies by up to a factor of six especially for low elevation angles. In the first simulation study, solely tropospheric delays were used as observations in the PPP analysis and coordinates, zenith delays and gradients were compared with the known values. The study has shown that the proposed approaches improve the ZTD accuracy to sub-mm level and decrease the errors in heights by approximately 70%. In the second simulation study, we generated simulated code and carrier phase observations and analyzed the observations using Bernese v5.2 based on PPP technique. The second simulation study has also shown that the proposed approaches decrease the errors of ZTD and heights. According to results of both simulation studies, it can be concluded that the approaches to modify the wet MF improve the accuracies of ZTD and height. It is important to note that the two simulation studies solely show us the potential improvements we can obtain in PPP. The assumption is that the NWM and all parameters derived from the NWM are error-free. In reality however, the NWM is not error-frees. We also carried out a real case study to show the performance of the approaches based on PPP technique using Bernese v5.2. The results show that the approaches decrease the ZTD errors in Germany and Türkiye. However, there is no improvement in heights especially for Türkiye. A possible explanation is that the NWM's accuracy is lower in Türkiye than in Germany. In summary, practically, the new approaches do not yield significant improvements in the estimated station coordinate. In fact, the approach based on climatology yields comparable results. This is in line with the results that were obtained with the newly developed VMF3 (Landskron and Böhm, 2018a). Although we improved the parameterization of the tropospheric delays, we measured this by comparing the difference between ray-traced and assembled delays, we do not find an improvement in PPP. We think that the reason can be related to the underlying data source that is used to estimate tropospheric parameters. In order to obtain tropospheric delays and additional parameters to apply proposed approaches, different NWM datasets can be used. We made use of ECMWF's ERA5 dataset which is globally available with high resolution both temporal and spatial. However, it is probably (to date) not accurate enough to apply for the derivation of tropospheric parameters related to the highly variable humidity field.

Acknowledgements

The authors are grateful to International GNSS Service (IGS) (Johnston et al., 2017), Center for Orbit Determination in Europe (CODE), Republic of Türkiye General Directorate of Land Registry and Cadastre (TKGM) for GPS data, precise orbits, clocks and global ionosphere maps. Ali Hasan Dogan was awarded '2214-A Abroad Research Scholarship' by The Scientific and Technological Research Council of Türkiye (TUBITAK) and accomplished his research at GFZ. The Fig. 1, 2 and 4 were plotted using the Generic Mapping Tools (GMT) (Wessel and Smith, 1998).

References

Bar-Sever, Y. E., Kroger, P. M., & Borjesson, J. A. (1998). Estimating horizontal gradients of tropospheric path delay with a single GPS receiver. *Journal of Geophysical Research: Solid Earth, 103*(B3), 5019-5035. doi: 10.1029/97JB03534.

Barriot, J. P., & Feng, P. (2021). *Beyond Mapping Functions and Gradients*. IntechOpen. doi: 10.5772/intechopen.96982.

Bevis, M., Businger, S., Herring, T. A., Rocken, C., Anthes, R. A., & Ware, R. H. (1992). GPS meteorology: Remote sensing of atmospheric water vapor using the global positioning system. *Journal of Geophysical Research: Atmospheres*, *97*(D14), 15787-15801. doi: 10.1029/92JD01517.

Böhm, J., & Schuh, H. (2004). Vienna mapping functions in VLBI analyses. *Geophysical Research Letters*, *31*(1), art. L01603. doi:10.1029/2003GL018984.

Böhm, J., Werl, B., & Schuh, H. (2006a). Troposphere mapping functions for GPS and very long baseline interferometry from European Centre for Medium-Range Weather Forecasts operational analysis data. *Journal of Geophysical Research: Solid Earth*, *111*(B2), art. B02406. doi:10.1029/2005JB003629.

Böhm, J., Niell, A., Tregoning, P., & Schuh, H. (2006b). Global Mapping Function (GMF): A new empirical mapping function based on numerical weather model data. *Geophysical Research Letters*, *33*(7), art. L07304. doi:10.1029/2005GL025546.

Böhm, J., Heinkelmann, R., & Schuh, H. (2007). Short note: a global model of pressure and temperature for geodetic applications. *Journal of Geodesy*, *81*(10), 679-683. doi: 10.1007/s00190-007-0135-3.

Chen, G., & Herring, T. (1997). Effects of atmospheric azimuthal asymmetry on the analysis of space geodetic data. *Journal of Geophysical Research: Solid Earth*, *102*(B9), 20489-20502. doi: 10.1029/97JB01739.

Dach, R., Lutz, S., Walser, P., & Fridez, P. (2015). *Bernese GNSS software version 5.2*. User manual, Astronomical Institute, University of Bern. ISBN: 978-3-906813-05-9.

Dach, R., Schaer, S., Arnold, D., Kalarus, M. S., Prange, L., Stebler, P., Villiger, A., & Jäggi, A. (2020). *CODE final product series for the IGS*. Astronomical Institute, University of Bern. doi: 10.7892/boris.75876.4.

Davis, J. L., Herring, T. A., Shapiro, I. I., Rogers, A. E. E., & Elgered, G. (1985). Geodesy by radio interferometry: Effects of atmospheric modeling errors on estimates of baseline length. *Radio science*, *20*(6), 1593-1607. doi: 10.1029/RS020i006p01593.

Hampel, F. R., Ronchetti, E. M., Rousseeuw, P. J., & Stahel, W. A. (2011). *Robust statistics: the approach based on influence functions*. John Wiley & Sons. ISBN: 978-1-118-15068-9.

Herring, T. A. (1992). Modeling atmospheric delays in the analysis of space geodetic data. *Proceedirws of Refraction of Transatmospheric simals in Geodesy, eds. JC De Munck and TA Spoelstra, Netherlands Geodetic Commission Publications on Geodesy*, *36*(4), 157-164.

Hersbach, H., Bell, B., Berrisford, P., Hirahara, S., Horányi, A., Muñoz-Sabater, J., ... & Thépaut, J. N. (2020). The ERA5 global reanalysis. *Quarterly Journal of the Royal Meteorological Society, 146*(730), 1999-2049. doi: 10.1002/qj.3803.

Jiao, D., Xu, N., Yang, F., & Xu, K. (2021). Evaluation of spatial-temporal variation performance of ERA5 precipitation data in China. *Scientific Reports*, *11*(1), art. 17956. doi: 10.1038/s41598-021-97432-y.

Johnston, G., Riddell, A., & Hausler, G. (2017). *The International GNSS Service*. Teunissen, Peter J.G., & Montenbruck, O. (Eds.), *Springer Handbook of Global Navigation Satellite Systems (1st ed., pp. 967-982)*. Cham, Switzerland: Springer International Publishing. doi: 10.1007/978-3-319-42928-1.

Landskron, D., & Böhm, J. (2018a). VMF3/GPT3: refined discrete and empirical troposphere mapping functions. *Journal of Geodesy*, *92*(4), 349-360. doi: 10.1007/s00190-017-1066-2.

Landskron, D., & Böhm, J. (2018b). Refined discrete and empirical horizontal gradients in VLBI analysis. *Journal of Geodesy, 92*, 1387-1399. doi: 10.1007/s00190-018-1127-1

Lyard, F., Lefevre, F., Letellier, T., & Francis, O. (2006). Modelling the global ocean tides: modern insights from FES2004. *Ocean dynamics, 56*, 394-415. doi: 10.1007/s10236-006-0086-x.

Masoumi, S., McClusky, S., Koulali, A., & Tregoning, P. (2017). A directional model of tropospheric horizontal gradients in Global Positioning System and its application for particular weather scenarios. *Journal of Geophysical Research: Atmospheres*, *122*(8), 4401-4425. doi: 10.1002/2016JD026184.

Niell, A. E. (1996). Global mapping functions for the atmosphere delay at radio wavelengths. *Journal of Geophysical Research: Solid Earth*, *101*(B2), 3227-3246. doi: 10.1029/95JB03048.

Niell, A. E. (2001). Preliminary evaluation of atmospheric mapping functions based on numerical weather models. *Physics and Chemistry of the Earth, Part A: Solid Earth and Geodesy, 26*(6-8), 475-480. doi: 10.1016/S1464-1895(01)00087-4.

Nilsson, T., Böhm, J., Wijaya, D. D., Tresch, A., Nafisi, V., & Schuh, H. (2013). Path delays in the neutral atmosphere. In *Atmospheric effects in space geodesy* (pp. 73-136). Springer, Berlin, Heidelberg. ISBN: 978-3-642-36931-5.

Rothacher, M., Springer, T. A., Schaer, S., & Beutler, G. (1998). Processing Strategies for Regional GPS Networks. In F. K. Brunner (Ed.), *Advances in Positioning and Reference Frames* (pp. 93–100). Berlin, Heidelberg: Springer Berlin Heidelberg. ISBN: 978-3-642-08425-6.

Rousseeuw, P.J., & Leroy, A.M. (1987). *Robust Regression and Outlier Detection*. John Wiley & Sons, New York. ISBN: 0–471–85233–3.

Saastamoinen, J. (1972). *Atmospheric correction for the troposphere and stratosphere in radio ranging satellites*. In Henriksen et al. (eds) *The use of artificial satellites for geodesy*, vol 15. AGU, Washington, pp. 247–251. doi: 10.1029/GM015p0247.

Santos, M. C., McAdam, M., & Böhm, J. (2012). Implementation status of the UNB-VMF1. *European Geosciences Union General Assembly 2012*, Vienna, 22-27 April 2012.

Steigenberger, P., Boehm, J., & Tesmer, V. (2009). Comparison of GMF/GPT with VMF1/ECMWF and implications for atmospheric loading. Journal of Geodesy, 83(10), 943-951. doi: 10.1007/s00190-009-0311-8.

Tesmer, V., Boehm, J., Heinkelmann, R., & Schuh, H. (2007). Effect of different tropospheric mapping functions on the TRF, CRF and position time-series estimated from VLBI. *Journal of Geodesy*, *81*(6), 409-421. doi: 10.1007/s00190-006-0126-9.

Teunissen, P. J., & Montenbruck, O. (2017). *Springer handbook of global navigation satellite systems*. New York, NY, USA: Springer. ISBN: 978-3-319-42926-7.

Thayer, G. D. (1974). An improved equation for the radio refractive index of air. *Radio Science*, *9*(10), 803-807. doi: 10.1029/RS009i010p00803.

Urquhart, L., Nievinski, F. G., & Santos, M. C. (2014). Assessment of troposphere mapping functions using three-dimensional ray-tracing. *GPS solutions*, *18*(3), 345-354. doi: 10.1007/s10291-013-0334-8.

van Dam, T., & Ray, R. (2010). S1 and S2 atmospheric tide loading effects for geodetic applications. *Available online:* https://geophy.uni.lu/atmosphere/tide-loading-calculator/ATM1OnlineCalculator/ (Accessed on 30 August 2022).

Velikou, K., Lazoglou, G., Tolika, K., & Anagnostopoulou, C. (2022). Reliability of the ERA5 in Replicating Mean and Extreme Temperatures across Europe. *Water*, *14*(4), art. 543. doi: 10.3390/w14040543.

Willis, P., Bar-Sever, Y.E., & Bock, O. (2012). *Estimating Horizontal Tropospheric Gradients in DORIS Data Processing: Preliminary Results*. In: Kenyon, S., Pacino, M., Marti, U. (eds) *Geodesy for Planet Earth. International Association of Geodesy Symposia, 136*. Springer, Berlin, Heidelberg. doi: 10.1007/978-3-642-20338-1_127.

Wessel, P., & Smith, W. H. (1998). New, improved version of Generic Mapping Tools released. *Eos, Transactions American Geophysical Union*, *79*(47), 579-579. doi: 10.1029/98EO00426.

Zhang, F., Barriot, J. P., Xu, G., & Hopuare, M. (2020). Modeling the slant wet delays from one GPS receiver as a series expansion with respect to time and space: Theory and an example of application for the Tahiti Island. *IEEE Transactions on Geoscience and Remote Sensing, 58*(11), 7520-7532. doi: 10.1109/TGRS.2020.2975458.

Zumberge, J. F., Heflin, M. B., Jefferson, D. C., Watkins, M. M., & Webb, F. H. (1997). Precise point positioning for the efficient and robust analysis of GPS data from large networks. *Journal of geophysical research: solid earth, 102*(B3), 5005-5017. doi: 10.1029/96JB03860.

Zus, F., Dick, G., Douša, J., Heise, S., & Wickert, J. (2014). The rapid and precise computation of GPS slant total delays and mapping factors utilizing a numerical weather model. *Radio Science*, *49*(3), 207-216. doi: 10.1002/2013RS005280.

Zus, F., Dick, G., Dousa, J., & Wickert, J. (2015). Systematic errors of mapping functions which are based on the VMF1 concept. *GPS Solutions*, *19*(2), 277-286. doi: 10.1007/s10291-014-0386-4

Zus, F., Douša, J., Kačmařík, M., Václavovic, P., Dick, G., & Wickert, J. (2019). Estimating the impact of global navigation satellite system horizontal delay gradients in variational data assimilation. *Remote Sensing*, *11*(1), art. 41. doi: 10.3390/rs11010041.

Zus, F., Balidakis, K., Dick, G., Wilgan, K., & Wickert, J. (2021). Impact of tropospheric mismodelling in GNSS precise point positioning: a simulation study utilizing ray-traced tropospheric delays from a high-resolution NWM. *Remote Sensing*, *13*(19), art. 3944. doi: 10.3390/rs13193944.

URL-1: Bos, M. S., & Scherneck, H. G. Free ocean tide loading provider. *Available online:* http://holt.oso.chalmers.se/loading/index.html (Accessed on 30 August 2022).